Journal of Power Sources 55 (1995) 143–152

Elasticity and electrical properties of porous bodies described as an agglomerate-of-spheres

H. Höpfinger, A. Winsel
Department of Physics, University of Kassel, Heinrich-Plett-Strasse 40, 34132 Kassel, Germany

Received 8 October 1994; in revised form 7 December 1994; accepted 10 December 1994

Abstract

The phenomenological characterization of a sintered, pressed or electrolytically produced porous body as an 'agglomerate-of-spheres' (AOS), estimated by the properties of their connections – the so-called necks–, was used to predict its break-force, elasticity and resistance. To this, the previous theoretical description of the AOS could be expanded by the definition of an ideal AOS. Furthermore, it could be shown, that the behaviour of the AOS is re-inforced by the relation of the radii of the sphere and neck. The description of the mechanical properties correlates well in the case of elasticity and break-tension with data of experiments at the University of Kassel with PbO_2-electrodes. The theoretically predicted values of the electrical properties are about a hundred times smaller than the experimental ones. This may be caused by the material-specific circuit capacity used for the PbO_2, since there are no data concerning the stoichiometric variance of the oxygen phase width in the neck region. An attempt to approach to real electrodes is only a trial, which, for the first time, takes experimental data into consideration. The lack of dependable material-specific sizes of lead dioxide is still the greatest inaccuracy in comparison with experimental data.

Keywords: Agglomate-of-spheres; Porous bodies

1. Introduction

An agglomeration-of-spheres (AOS) represents an aggregate of spherical particles, connected by the so-called necks (Fig. 1). The phases of spheres and necks are distinguished by different Laplace pressures, a stoichiometric variance, δ, of the phase width of the chemical compounds [1] and a resulting potential difference [2]. The geometric structures of spheres and necks can be based on these values [2]. Some phenomena of macroscopic samples could already be derived phenomenologically by the AOS model, for example:

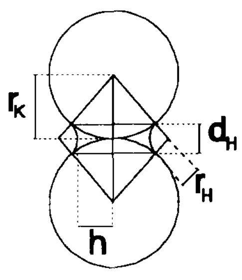

Fig. 1. Two spheres connected with a neck.

- the circuit-capacity behaviour of different samples during sintering
- the protection of the necks against corrosion, caused by thermodynamic 'underpotential deposition' [2]
- the diagnosis of the 'antimony-free effect' as a result of a 'relaxable insufficient mass utilization', as well as a therapy against the cycle-dependent constant capacity loss [2]
- the behaviour of lead-traction batteries [3]

The mentioned examples came from closer investigation of the base units of such a system. These base units can be used to construct an ideal AOS. Theoretical examinations of the structure and look of an ideal agglomerated of spheres give a better understanding of the elasticity, resistance and break-force of macroscopic bodies. All investigations carried out are of general significance, but the choice of outer frames are related to the experiments started at the University of Kassel with an experimental setup for the determination of different mechanical and electrical properties of PbO_2 electrodes [4]. With this, the relevance of the model and changes carried out should be verifiable, while calculations are fixed.

SSDI 0378-7753(95)02181-F

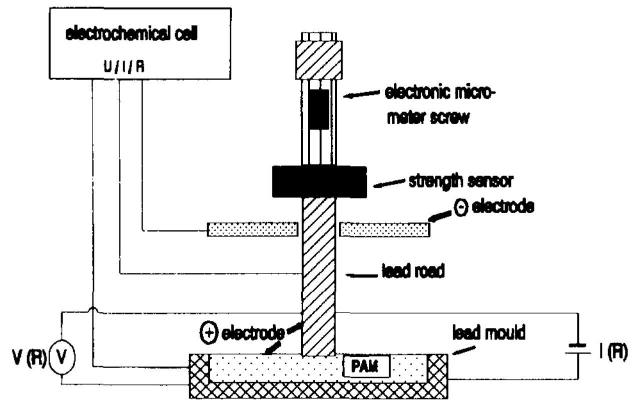

Fig. 2. Schematic picture of the experimental setup.

Table 1
Porosity and package density of different lattices

	Package density	Porosity
Simple cubic	0.52	0.48
Face-centred cubic	0.68	0.32
Body-centred cubic	0.74	0.26

2. Experimental

The experiment [4], as schematically shown in Fig. 2, is meant to fabricate lead dioxide electrodes. The whole setup stays in a solution of sulfuric acid up to the negative electrode, while the electrodes are formed by charging the lead paste tablets.

After cycling, the structure of the electrodes will be formed as an AOS, which is connected to the lead mould with a stamp and bowl.

Analyses is done by varying the number of charge and discharge cycles, the way of producing the tablets, the velocity of expansion as well as the two shapes of the electrodes.

On shape is called 'bowl-like', when the tablet is connected to the lead mould as shown in Fig. 2, while the other one only has contact to the sidewalls and is called 'membrane-like'.

3. Ideal AOS

Ideal AOS consists of small, periodically arranged, spherical particles. There are neither missing nor have interim positions.

Table 1 [3] shows the porosity and package density of different lattices.

The choice of the ideal structure is the simple cubic arrangement with porosity 0.48 (which is close to the porosity of the lead accumulator electrodes [3–6]. In addition, each sphere has six neighbours and each contact zone has a neck.

4. Expansions and approximations

The elasticity of the neck between two spheres due to $h \ll r_K$, determines the properties of the AOS. The spheres are inelastic.

All deformations of the necks may be described either as expansion or shear. Due to their position, all necks exposed to equal forces are gathered. The elasticity of the necks can be described by a coefficient of extension (CE), which then can be combined as parallel or serial springs. The shape of the macroscopic bodies is close to that, used in the experiment. For reasons of approximation, these samples will be divided into two areas; they can be treated independently. The aim is to get a more homogeneous distribution of the forces.

5. Effective thickness of the neck

Out of a geometric view, according to Fig. 3, it can be shown, that the thickness, d_H, of the neck, from where the radius of the sphere arises, is derived from:

$$(r_K + r_H)^2 = (h + r_H)^2 + r_K^2 \tag{1}$$

and,

$$\frac{d_H}{2r_H} = \frac{r_K}{r_K + r_H} \tag{2}$$

can be written as:

$$d_H = \left(\frac{1}{2r_K} + \frac{r_K - \sqrt{2r_K \sigma \epsilon^{-1}}}{2r_K \sigma \epsilon^{-1}}\right)^{-1} \tag{3}$$

6. Base elements

The macroscopic AOS will be described as 'base-units', which are determined by the behaviour of the neck.

The values, which determine the mechanical properties, are the CE of a neck referring to the extension D_D, the shearing D_S and their combination D_{DS}. The electric behaviour is also re-inforced by the neck, although the important parameter is not the geometric

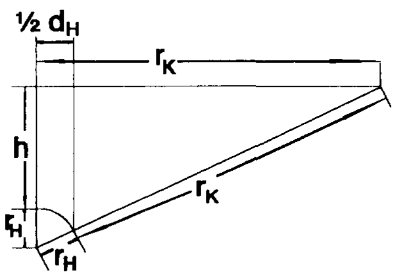

Fig. 3. Description of the effective thickness of a neck d_H.

resistance, but the so-called constriction resistance, which arises from the theory of electric contacts.

6.1. Basing mechanical units

For the CE of an extended neck D_D is [7]:

$$D_D = \frac{F}{\Delta l} = \frac{\epsilon E A_H}{\Delta l} = \frac{E A_H}{d_H} \tag{4}$$

where F is the force, E the module of elasticity, ϵ the specific extension, and A_H the cross-section of the neck (Fig. 4). The thrust, τ, of a sheared neck is [7]:

$$\tau = \frac{F}{d_H^2} = G \tan \vartheta \tag{5}$$

With the definition of the module of the thrust G [8] and the cross tension μ [7]:

$$G = \frac{E}{2(1-\mu)}$$

and,

$$\mu = \frac{d_H}{\Delta d_H} \frac{\Delta h}{h} \tag{6}$$

comes for the CE of a sheared neck:

$$D_S = \frac{F}{\Delta l} = \frac{E d_H}{2(1+\mu)} \tag{7}$$

Since in one base-unit with nonparallel shift of neighbouring necks both the tension and the shearing occur parallel to one another, a combined parameter can be used:

$$D_{DS} = D_D + D_S = \frac{E A_H}{d_H} + \frac{E d_H}{2(1+\mu)} \tag{8}$$

6.2. Basing electrical units

The geometrically determined resistance, R_G, of a neck is given as:

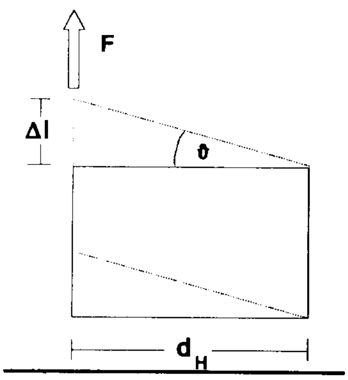

Fig. 4. Shearing of a cylindric neck.

$$R_G = \rho \frac{d_H}{A_H} \tag{9}$$

where, ρ is the specific resistance.

In the case of a sphere of about 1 μm, and a neck, which is about factor six smaller, an additional effect appears, the constriction resistance, R_E. This term leads back the higher constriction resistance to the constriction of the current flow in the necks. Holm [9] determined this parameter with a model of a constriction between two never-ending isolating layers according to Fig. 5 [10].

The relation of these resistances gives:

$$\frac{R_E}{R_G} = \frac{\pi}{2} \left(\frac{r_K}{h} + \frac{h}{2r_K} - 1 \right) \tag{10}$$

This ratio is, according to the relation of the radius of sphere and neck, 6:1 [2]. Therefore, only the constriction resistance has to be taken into consideration.

From the definition of the cross tension, μ [7], the change of the radius as a function of the force results in:

$$\Delta h = \frac{\mu h F}{d_H D_D} \tag{11}$$

The resistance, R_H (F) of a neck is:

$$R_H(F) = \frac{\rho}{2(h - \Delta h)} = \frac{\rho}{2h\left(1 - \dfrac{\mu F}{d_H D_D}\right)} \tag{12}$$

Only negligible changes of the resistance occur in the case of shearing. As the tension only enters into the geometric resistance, the change needs to be several times higher than the beginning state in order to be effective, which one cannot expect.

The coupled sizes of extension and shearing allow an estimating of the maximal changes of the cross-area.

$$\tan \vartheta = \frac{\Delta l}{d_H} = \lambda \tag{13}$$

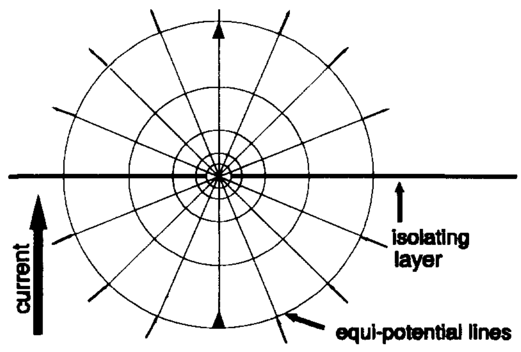

Fig. 5. Model to describe the current distribution and equi-potential surfaces.

With the help of the so-called 0.3% tension, commonly used for metals, the relation of the areas of the beginning and minimum state A_0 and $A_{\min}$ gives:

$$\frac{A_0}{A_{\min}} \approx \frac{1}{\cos^2 \vartheta} \tag{14}$$

This relation is very close to 1.

7. Break force

A_I is the expected area where the sample will break, at the contact of stamp and AOS. A_I consists of n_{Ip} parallel necks, which can be described by the CE D_{I1} of a monolayer with:

$$D_{I1} = n_{Ip} D_D = \frac{A_I}{A_R} D_D = \frac{\pi r_I^2}{4 r_K^2} D_D \tag{15}$$

where A_R is the area with side-length $2r_K$, needed for one sphere.

The material-specific break-tension λ gives the value of the specific tension ϵ, and the sample will therefore break. The force F_z therefore is [7]:

$$F_Z = \lambda d_H D_{I1} = \lambda d_H D_D \frac{\pi r_I^2}{4 r_K^2} \tag{16}$$

8. The bowl-like AOS

For the bowl-like AOS (Figs. 6 and 7), it is approximately valid, that:

- (I) and (II) can be treated independently
- in (I) only extension occurs

For the electrical properties it is valid, that:

- in area (I) all currents through the chains in the direction of the force are the same and out of that, all of the cross-wise necks are currentless.

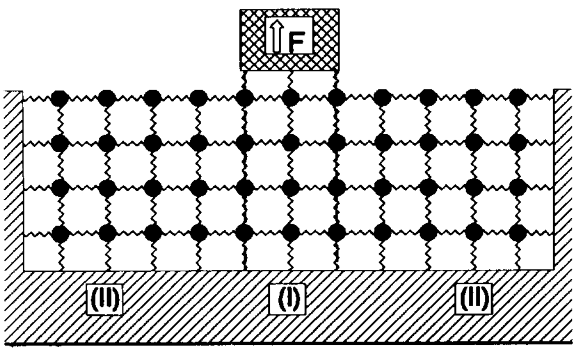

Fig. 6. Schematic view of a bowl-like AOS.

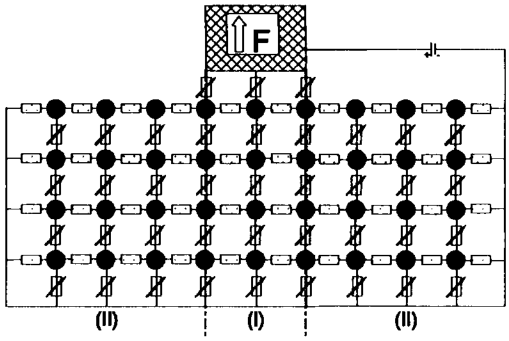

Fig. 7. Substitutional circuit diagram of a bowl-like AOS.

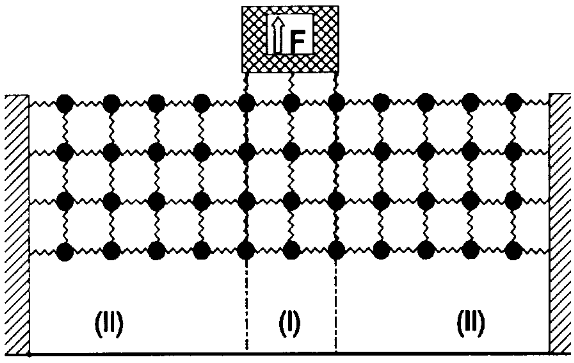

Fig. 8. Schematic view of a membrane-like AOS.

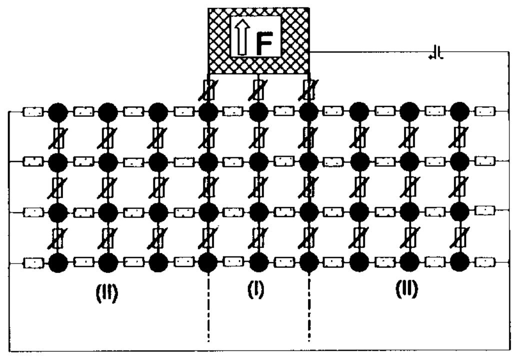

Fig. 9. Substitutional circuit diagram of a membrane-like AOS.

9. The membrane-like AOS

In the case of the membrane-like AOS (Figs. 8 and 9), the approximations are, that:

- each neck vertical to the force in area (II) gets extended, as soon as an extension Δl occurs
- all the necks in area (II) in the direction of the force get sheared
- at the sides of area (I) an extending force is effective, which will be neglected; area (I) has no contribution to the mechanical and electrical behaviour of the membrane.

10. Elasticity of the bowl-like AOS

The elasticity of area (I), D_I is given by n_{Ip} parallel chains with the length d. Their D_K is:

$$D_K = \frac{2r_K D_D}{d} \tag{17}$$

For region (I) it will be:

$$D_I = n_{Ip} D_K = \frac{A_I D_D}{2r_K d} = \frac{A_I E A_H}{2r_K \, d \, d_H} \tag{18}$$

The CE of one neck is, determined by length and cross section:

$$D_D = \frac{F}{\Delta l} = \frac{E A_H}{d_H} \tag{19}$$

In area (II) a more distinguishing view is necessary. A summation of all necks, that lie on equi-potential surfaces according to Figs. 10 and 11, will serve for the description of these serial-connected layers. The area of the first equi-potential surface is appropriate to the surface of a quarter of a torus:

$$A_1 = \pi^2 r_I r_K \tag{20}$$

and for the nth area:

$$A_n = \pi^2 r_I r_K (2n-1) \tag{21}$$

The CE of the whole area(II) can be written as a summation over the n layers where an approximation of the start- and endpoints is necessary.

Since the change in a sufficient distance of the stamp is not worth mentioning, the value of n_d will be used as the maximum level. An estimation of the relation of the CE for $n=1$ and $n=n_d$ results to 1:2000.

The CE of the nth layer is:

$$D_n = n_n D_{DS} = \frac{A_n}{A_R} D_{DS} \tag{22}$$

Summation of the n serial layers gives:

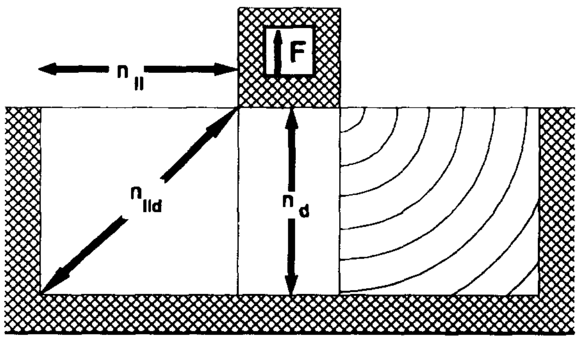

Fig. 10. Equi-potential lines of force and the number of layers in each direction.

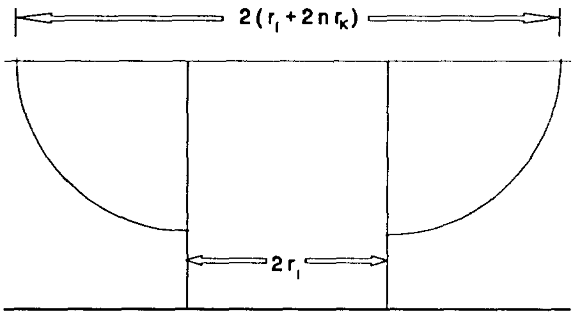

Fig. 11. Description of the cross section of one equi-potential layer.

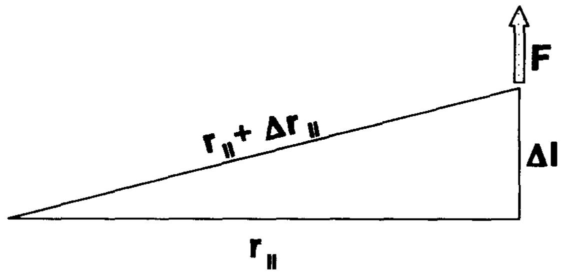

Fig. 12. Geometric view for Eq. (25).

$$D_{II} = \frac{1}{\sum_n \frac{A_R}{A_n D_{DS}}} \tag{23}$$

Setting in for A_n and the limiting values

$$D_{II} = \frac{D_{DS} \pi^2 r_I}{4 r_K} \left(\sum_{n=1}^{n_{II}} \frac{1}{(2n-1)} \right)^{-1} \tag{24}$$

11. Elasticity of the membrane-like AOS

The length Δl comes from:

$$\Delta l = \sqrt{(r_{II} + \Delta r_{II})^2 - r_{II}^2} = \frac{F}{D_M} \approx \frac{F}{D_{II}} \tag{25}$$

since area(I) has a negligible influence (Fig. 12). The result is an extension- or force-dependent CE:

$$D_M = \frac{F}{\sqrt{\left(r_{II} + \frac{F}{D_{II}}\right)^2 - r_{II}^2}} \tag{26}$$

A summation of all necks that receive the same force is also necessary to describe the area (II) of the membrane-like AOS.

The equi-potential surfaces are now hollow cylinders with the thickness of $2r_K$. The number of spheres in one cylinder with radius $r_I + r_K$, in which the first spheres lie:

$$n_{HI} = \frac{n_d \pi d (r_I + r_K)}{r_K} \tag{27}$$

The CE of the nth hollow cylinder D_{Hn} then is:

$$D_{Hn}=n_{Hn}D_{DS}=\frac{\pi D_{DS}d}{2r_K^2}\left[\sum_{n=1}^{n_{II}}\frac{1}{r_I+r_K(2n-1)}\right]^{-1} \tag{28}$$

Substituting for D_{II}:

$$D_M(F)=F\left[\left(r_{II}+F\frac{\pi dD_{DS}}{2r_K^2}\sum_{n=1}^{n_{II}}\frac{1}{r_I+r_K(2n-1)}\right)^2-r_{II}^2\right]^{-1/2} \tag{29}$$

The result is only a context between the outer dimensions, the size of the spheres and the elasticity of their compounds.

12. Electrical properties of the bowl-like AOS

12.1. Resistance of area (I)

Since area (I) only consists of n_{Ip} parallel chains with the length d and the resistance R_K of one chain, it can be written as:

$$R_I=\frac{1}{n_{Ip}}R_K=\frac{2dr_K}{A_I}R_H \tag{30}$$

for area (I):

$$R_I=\frac{2dr_K}{A_I}R_H(F)=\frac{dr_K}{A_Ih}\frac{\rho}{1-\dfrac{\mu F}{d_Hn_{Ip}D_I}} \tag{31}$$

12.2. Resistance of area (II)

The torus-formed layers are again useful to summarize the necks exposed to the same effect of the force, similar to the description of the mechanical properties of area (II). The start- and endpoints of the summation are again close to the data given in Fig. 10.

Area (II) can be described by the summation of n serial layers as:

$$R_{II}=\sum_{n=1}^{n_d}\frac{R_HA_R}{A_n}=\sum_{n=1}^{n_d}\frac{4R_Hr_K}{\pi^2r_I(2n-1)}=\sum_{n=1}^{n_d}\frac{2r_K}{\pi^2r_I(2n-1)}\frac{\rho}{h\left(1-\dfrac{2\mu Fr_K}{d_HD_{II}\pi^2r_In_d}\right)} \tag{32}$$

Therefore, the resistance of the whole bowl-like AOS as a function of the force is:

$$R_W(F)=\frac{dr_K}{A_Ih}\frac{\rho}{1-\dfrac{\mu F}{d_Hn_{Ip}D_I}}+\frac{2r_K}{\pi^2r_Ih}\sum_{n=1}^{n_d}\frac{1}{2n-1}\frac{\rho}{1-\dfrac{2\mu Fr_K}{d_HD_{II}\pi^2r_In_d}} \tag{33}$$

13. Electrical properties of the membrane-like AOS

13.1. Resistance of area (II)

Since area (I) will be negligible, area (II) can be divided into hollow cylinders with the thickness of $2r_K$, with n_{Hn} parallel spheres each.

The resistance of the serial connected layers is:

$$R_{II}=\sum_{n=1}^{n_{II}}\frac{R_H}{n_{Hn}}=\sum_{n=1}^{n_{II}}\frac{2R_Hr_K^2}{\pi d(r_I+r_K(2n-1))} \tag{34}$$

Setting in for R_H gives the resistance of the membrane-like AOS:

$$R_M(F)=\frac{r_K^2\rho}{\pi dh}\sum_{n=1}^{n_{II}}\left\{[r_I+r_K(2n-1)]\times\left[1-\frac{2\mu Fr_K^2}{d_HD_M\pi d(r_I+r_K(n_{II}-1))}\right]\right\}^{-1} \tag{35}$$

14. Approximation to real electrodes

The porosity, often determined in a gravimetric way, disregards the variation of the size of the particles or necks.

Scanning electron microscope (SEM) pictures [11] show that in the case of real electrodes many spheres – in favor of bigger particles – are 'missing' and necks are often not produced. This is important, as only the neck is determining the calculations, and such a situation would lead to higher elasticity, as only the number of necks per area decreases or fewer material is used to build the necks.

With the help of SEM pictures of the 'tear' surface of dried PbO_2 electrodes (see Figs. 13 and 14) the necks were counted manually at a magnification up to 1:3000.

As a first approach to real electrodes, a density of necks can be given. For comparison with theoretical values, this will be used as a multiplicative form factor α:

$$\alpha=\frac{n_{build}}{n_{ideal}} \tag{36}$$

The ideal and determined density is:

$$n_{ideal}=\frac{n}{A_R}=\frac{1}{4r_K^2}=2.5\times10^{11}\frac{1}{m^2}$$

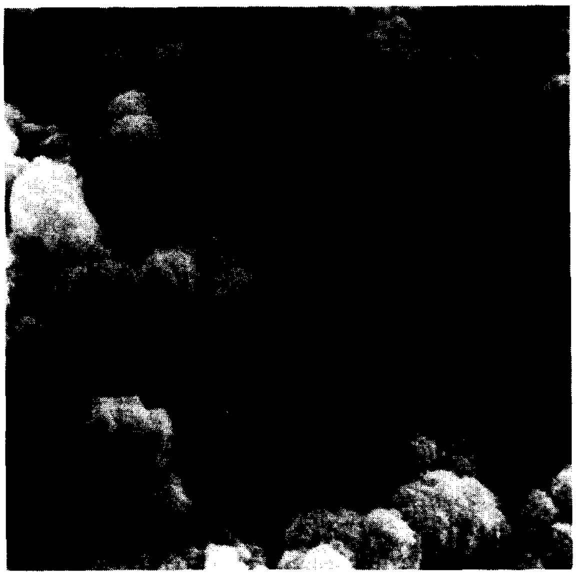

Fig. 13. Scanning electron microscope picture of a teared PbO_2 electrode [4], magnification ×1000.

Fig. 14. Scanning electron microscope picture of a sintered cobalt sample [10], magnification ×1000.

and,

$$n_{\mathrm{build}} = 1.8 \times 10^{11}\ \frac{1}{m^2}$$

and $\alpha \approx 0.7$

15. Results and comparison with experimental data

The experimental values, used in the following chapters are [4]:

$r_{\mathrm{I}} = 4.988 \times 10^{-3}$ m

$r_{\mathrm{II}} = 20.25 \times 10^{-3}$ m

and,

$d = 2.8 \times 10^{-3}$ m

The material specific values are:

$\sigma = 1$ J/m^2 [12]

$\mu = 0.25 \pm 0.05$ [13]

$\epsilon_0 \approx 7 \times 10^7$ J/m^2 [2]

$\rho = (2.9 \pm 0.05) \times 10^{-6}\ \Omega$ m [14]

and

$E = (3 \pm 2) \times 10^7$ N/m^2 [13]

As no value could be found for the specific break-tension λ of compact PbO_2, the so-called 0.3% tension [15], commonly used for metals, is used to determine the break-force. The form factor α is only given to show tendencies, as it is just the first approach to a real 'AOS'.

16. Mechanical properties

The CE of the bowl-like AOS comes to:

$D_{\mathrm{W}} = 1.34 \times 10^6\ N/m$

and,

$D_{\mathrm{W}\alpha} = 9.4 \times 10^5\ N/m$

The course of the extension- or force-dependent CE of the membrane-like AOS behaves as shown in Fig. 15.

The break-force with the 0.3% tension gives:

$F_{\mathrm{Z}} = 16$ N

and,

$F_{\mathrm{Z}\alpha} = 11$ N

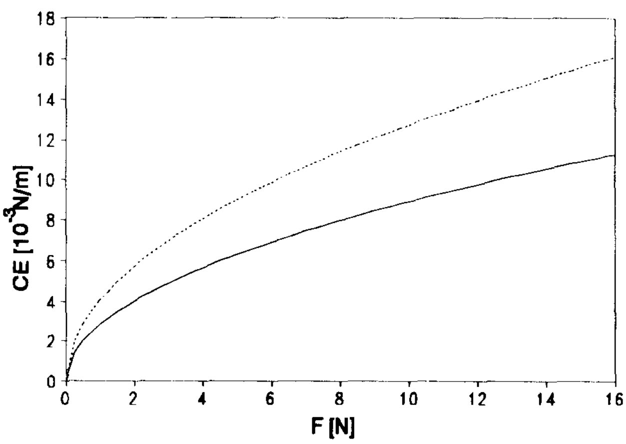

Fig. 15. Calculated constant of extension of the membrane-like AOS (——); with form-factor correction (····).

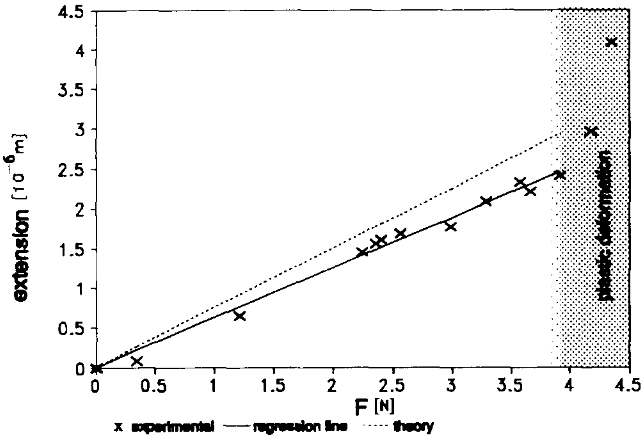

Fig. 16. Measured [4] and calculated data of a bowl-like AOS.

This correlates well with early experiments, that came to $F_Z \approx 14$ N, while more recent analysis give $F_Z \approx 10$ N.

16.1. Comparison of the mechanical properties of a bowl-like AOS

Fig. 16 represents the measured and calculated CE of the bowl-like AOS. The gradient of the regression line of the first 12 measuring points comes to $D_{MREG} = 1.593 \times 10^6$ N/m (the coefficient of regression is ≈ 0.988). The region in the measured curve, where plastic deformation starts, cannot be described with the model. The end point of the proportional behaviour could also be at $F \approx 2.5$ N, $F \approx 4$ N would then be the yield point. But this does not seem the case, since this would lead to a very small break-force. In earlier experiments the break-force was about 14 N, while recent experiments give a value of about 10 N. This correlates well with the calculations of $F_Z = 16$ N or rather $F_{Z\alpha} = 11$ N, when corrected with the form-factor.

17. Electrical properties

The resistance of the unloaded AOS (Figs. 17 and 18) is:

$R_W(0) = 5 \times 10^{-4}\ \Omega$

and,

$R_M(0) = 1.3 \times 10^{-3}\ \Omega$

18. Discussion

The approximations are:

(i) due to the relation of h versus r_K, the mechanical and electrical properties of the spheres have been neglected;

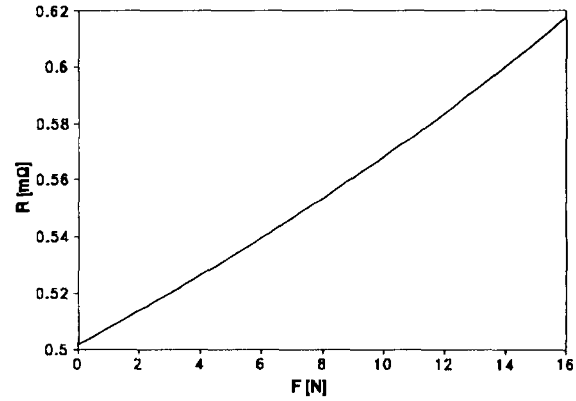

Fig. 17. Resistance of the bowl-like AOS as a function of force.

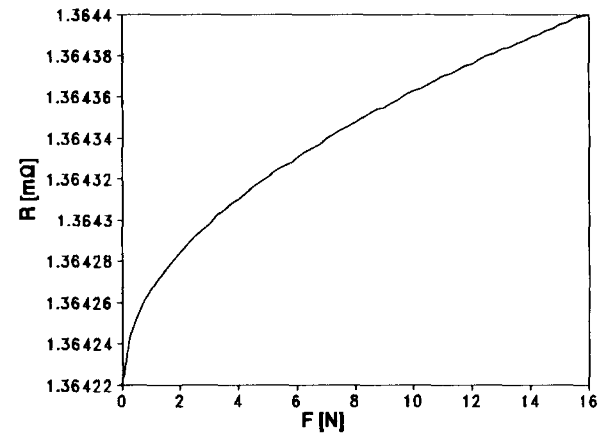

Fig. 18. Resistance of the membrane-like AOS as a function of force.

(ii) rough estimation of the effective thickness d_H of the neck, as the transition of neck and sphere is continuous, and

(iii) only in tendency assessable faults by acceptation of independent-treatable areas (I) and (II).

In this theoretical AOS model, the electrolyte has not been taken into consideration. This probably smaller elasticity was disregarded at all, in addition to cohesion- and viscosity-forces. This does not cause any remarkable fault in the case of the electrical forces, as the circuit capacity of PbO_2 is about 5000 times higher than that of the electrolyte at a normal concentration of 7 M.

One fundamental problem is the absence of sufficiently examined material parameters. This lack of reliable information on PbO_2, already remarked by Thomas [14] in 1948, is still valid.

The existence width δ of the $PbO_{2-\delta}$ has been examined by Pohl and Rickert [1], but to date nothing is known on the change of the mechanical or electrical properties of PbO_2. The parameters published in the literature already differ a lot, the phase-width has not yet been taken into consideration.

This is also true for the break-experiment, as the break-force determined with the 0.3% tension could, besides the brittleness of the PbO_2, be higher.

It is necessary to mention that the quality of the formation of the AOS-structure, is not yet fully understood.

Due to the long formation cycles, there is not yet any statistically data available from which an optimal formation process can be derived in order to get reproducible structures of AOS.

19. View

For comparison with theoretically determined values, a change of the break-experiments with regard to geometrically simple bodies could give more exact statements. One possible form is that of the rod-like structure, which is distinguished by higher homogeneity referring to the distribution of force and current, and excludes area (II), defined by rougher approximations. Furthermore, the insufficient knowledge on the current distribution at the contact zones during formation could better be excluded.

The influence of the number of charge and discharge cycles on the capacity of a lead accumulator is known as an 'afe' (antimony-free effect). This effect, which is afflicted with a constant capacity loss per cycle [16] could be examined by varying the number of cycles before stressing.

The experiments, time consuming, could be changed in such a way that the electrode is only somewhat extended and then is recycled. The stamp could be brought into the normal position after a short extension, such that no lasting change in the structure of the AOS is suspected.

A comparison of the theoretical models with other than electrolytically produced porous bodies, (e.g., sintered ones) should also be examined.

The attempt of making predictions, started in this work, could help finding more information on the specific mechanical and electrical properties of PbO_2.

20. List of symbols

A_1	$\frac{1}{4}$ of the surface of the first torus
A_H	cross area of one neck
A_f	area of the stamp
A_K	cross area of one sphere
A_{min}	cross area of one neck under maximum strength
A_n	$\frac{1}{4}$ of the surface of the nth torus
A_{nd}	area of the torus with $n=n_d$
A_R	quadratic area around one sphere
d	thickness of the sample
D_B	constant of extension of a solid body
D_D	constant of extension of an extended neck
D_{DS}	constant of extension of the combination of extension of one and shearing of another neck
D_{GES}	constant of extension of the whole AOS
d_H	effective thickness of the neck between two spheres
D_{Hn}	constant of extension of the nth hollow cylinder
D_I	constant of extension of area (I)
D_{I1}	constant of extension of a monolayer of spheres/necks with the area A_I
D_{II}	constant of extension of area (II)
D_K	constant of extension of a chain necks
D_M	constant of extension of the membrane-like AOS
$D_{M\alpha}$	constant of extension of the membrane-like AOS under the consideration of the form-factor α
D_{MERG}	gradient of the regression line of one measurement
D_n	constant of extension of the necks of the nth surface of a torus
D_S	constant of extension of a sheared neck
D_W	constant of extension of the bowl-like AOS
$D_{W\alpha}$	constant of extension of the bowl-like AOS under consideration of the form-factor α
E	module of elasticity
F	force
F_Z	force, which is necessary to tear a monolayer of necks with the area A_I
G	module of shearing
h	radius of neck
h_{min}	radius of the neck under maximum stress
n_d	number of spheres referring to the thickness of the sample
n_{build}	number of necks per area determined by counting
n_{H1}	number of spheres in the first hollow cylinder
n_{Hn}	number of spheres in the nth hollow cylinder
n_{ideal}	number of necks per area (according to Section 14)
n_{II}	number of spheres in a chain with the length r_{II}
n_{IId}	number of spheres in the direction according to Fig. 10
n_{Ip}	number of parallel chains in area (I)
n_n	number of spheres in a quarter of the nth surface of a torus
p	pressure
P	porosity
P_H	Laplace pressure of the neck
P_K	Laplace pressure of the sphere
R_B	resistance of a solid body
R_G	geometric electric resistance of a neck
r_H	radius of the throat of a neck
R_H	resistance of a neck

r_{I}	radius of area (I)
R_{I}	resistance of area (I)
r_{II}	radius of area (II)
R_{II}	resistance of area (II)
r_{K}	radius of a sphere
R_{K}	resistance of a chain of necks
R_{KD}	resistance of n_{d} parallel chains with the resistance R_{K}
R_{M}	entire resistance of the membrane-like AOS
r_{PR}	entire radius of the sample
R_{W}	entire resistance of the bowl-like AOS
$U(r_{\mathrm{I}})$	circumference of a circle with radius r_1
U	circumference
$\bar{U}$	half the circumference of area (II)
V	volume
V_{K}	volume of a sphere

Greek letters

α	form-factor
Δl	extension, change of length
Δr_{II}	change of the length of the radius r_{II} according to Fig. 12
η	density
ϵ	specific extension $\Delta l/l$, universal
ϵ_0	flow-tension
ϵ_{D}	specific extension of a neck of one volume element of a sphere
ϵ_{DB}	specific extension of a solid body
ϵ_{DS}	specific extension and shearing of a neck
ϵ_{S}	specific shearing of one neck
ϵ_{SB}	specific shearing of a solid body
λ	specific break-tension
μ	constant of cross contraction
ϑ	angle of shearing
ρ	specific resistance
σ	surface strength
τ	thrust

References

[1] J.P. Pohl and H. Rickert, in S. Trassatt (ed.), *Electrodes of Conductive Metallic Oxides,* Elsevier, Amsterdam, 1980.

[2] A. Winsel, E. Voss and U. Hullmeine, *J. Power Sources, 30* (1990) 209–226.

[3] W.G. Geuer, Untersuchungen über das Alterungsverhalten von Blei Akkumulatoren, *Thesis,* University of Aachen, Germany, 1991.

[4] E. Bashtavelova and A. Winsel, *J. Power Sources, 46* (1993) 219–230.

[5] P. Lürkens, Untersuchungen an leistungssteigernden Massnahmen für den Bleiakkumulator, *Thesis,* University of Aachen, Germany, 1989.

[6] C.D. Drotschmann, *Bleiakkumulatoren,* Verlag Chemie, Weinheim/Bergstr., Germany, 1952.

[7] B.M. Jaworski and A.A. Detlaf, *Physik Griffbereit,* Vieweg, Braunschweig, Germany, 1972.

[8] C.G. Gerthsen, H.O.K. Kneser and H.V. Vogel, *Physik,* Springer, Berlin, 14th edn., 1982.

[9] R. Holm, *Electric Contacts,* Springer, Berlin, 1958.

[10] B. Willer, Elektrische Leitfähigkeit und Dilatation bei Sintervorgängen, *Thesis,* University of Kassel, Germany, 1984.

[11] V.E. Rückborn, A. Winsel and B. Willer, *DECHEMA-Mongr., 102* (1986) 513–543.

[12] *Handbook of Chemistry and Physics,* CRC, 56th edn., Boca Raton, FL, 1975.

[13] *Gmelins Handbuch der anorganischen Chemie, Lead: Part 47/ C1,* Verlag Chemie, Weinheim/Bergstr., Germany, 1969.

[14] U.B. Thomas, *The Electrical Conductivity of Lead Dioxide,* Bell Telephone Laboratories, Murray Hill, NJ, USA, 1984.

[15] G. Guy, *Metallkunde für Ingenieure, Technisch-Physikalische Sammlung, Vol. 7,* Akademische Verlagsgesellscahft, Frankfurt/ Main, Germany, 1970.

[16] E. Meissner and E.V. Voss, *J. Power Sources, 33* (1991) 231–244.